nature communications

Article

https://doi.org/10.1038/s41467-024-53508-7

Diversities of chromite mineralization induced by chemo–thermal evolution of the mantle during subduction initiation

Received: 3 September 2023

Accepted: 11 October 2024

Published online: 30 October 2024

Check for updates

Peng-Fei Zhang[1] ✉, Mei-Fu Zhou[1] ✉, Paul T. Robinson[1], John Malpas[2], Graciano P. Yumul Jr.[3], Christina Yan Wang[4] & Jie Li[5]

Ophiolites, mostly formed via subduction initiation at proto-forearcs, exhibit a unique variation of mantle-derived magmatism from MORB-like to low-Ti tholeiitic and boninitic-like affinities. Such variation was suggested to form chromite deposits spanning high-Al to high-Cr types. Nevertheless, the origin of diverse magmatism during subduction initiation and their linkages to different chromite deposits has long been enigmatic. Here we show elemental and Os isotopic compositions of different chromitites from the Zambales ophiolite, Philippines. Combined with data from ophiolites worldwide, high-Al and high-Cr chromitites are revealed to result from low-Ti tholeiitic and boninitic-like magmatism, respectively. Proto-forearc mantle had few chromitites generated during MORB-like magmatism, but afterwards, it was modified first by slab fluids and later by continuous asthenospheric upwelling in the context of slab densification and rollback. The latter modification elevated the geothermal gradient and replenished fertile components in the proto-forearc mantle progressively, inducing increasingly higher degrees of mantle melting and Cr-richer magmatism and chromitites.

Podiform chromite deposits are an exclusive feature of ophiolites and constitute important sources of chromium and refractory materials[1]. Chromite grains in such deposits exhibit a wide range of Cr# (100 × Cr/(Cr + Al); 3–85; Fig. 1), which allows the division of the deposits into high-Al (Cr# < 60) and high-Cr (Cr# > 60) varieties[1,2]. Traditionally, high-Al chromitites are thought to be formed from MORB-like magmas that originated from the fertile asthenospheric mantle below spreading ridges, whereas high-Cr chromitites were formed from boninitic-like magmas generated via flux melting of the depleted mantle in subduction settings[3–5]. However, such explanations contradict our compiled geological evidence that ophiolites which host high-Cr chromitites mostly contain lherzolites and Cpx-rich harzburgites in their mantle sequences (Fig. 1 and Supplementary References), suggesting that the mantle fertility during the formation period of high-Cr chromitites was not as poor as previously assumed. Moreover, ophiolites containing exploitable high-Cr chromite deposits often have high-Al chromitites, whereas those with high-Al deposits have few high-Cr chromitites, a feature which has been widely reported but rarely further considered yet (Fig. 1). These observations indicate that the origins of ophiolitic chromite deposits are far more intricate than generally thought, and further investigation is required to clarify the cause of diverse chromite mineralization in ophiolites and their mutual genetic linkages.

Ophiolites that host chromite deposits, e.g. the Troodos (Cyprus), Semail (Oman), and Zambales (Philippines) ophiolites, often show a chemo–stratigraphic variation trend comparable to the infant West

[1]State Key Laboratory of Geological Processes and Mineral Resources, China University of Geosciences, Wuhan, China. [2]Department of Earth Sciences, The University of Hong Kong, Hong Kong, China. [3]Cordillera Exploration Company, Inc., NAC Tower, BGC, Taguig City, Philippines. [4]CAS Key Laboratory of Mineralogy and Metallogeny, Guangzhou Institute of Geochemistry, Chinese Academy of Sciences, Guangzhou, China. [5]State Key Laboratory of Isotope Geochemistry, Guangzhou Institute of Geochemistry, Chinese Academy of Sciences, Guangzhou, China. ✉e-mail: zhangpengfei073061@163.com; zhoumeifu@hotmail.com

https://doi.org/10.1038/s41467-024-53508-7

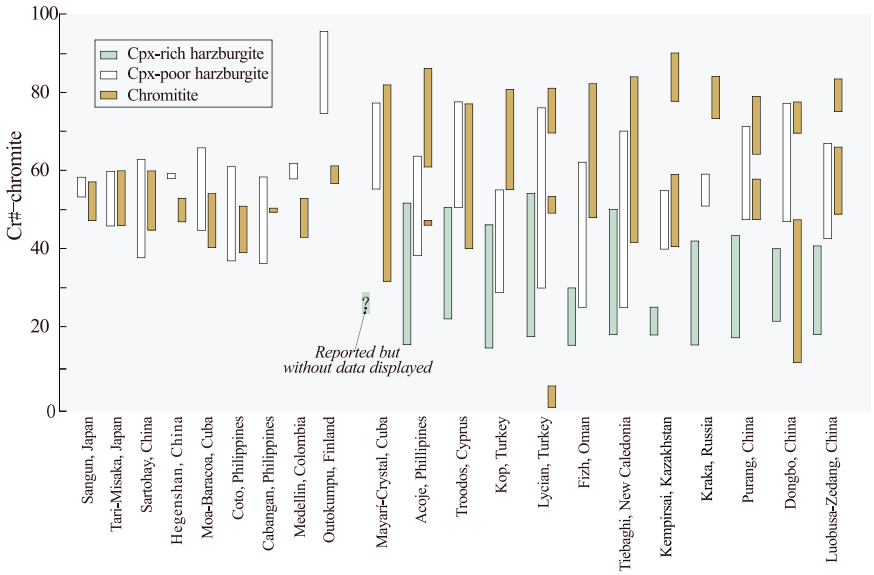

Fig. 1 | Variation of Cr# of chromite in peridotites and chromitites from ophiolitic blocks that contain chromite deposits. Peridotites in blocks that only host high-Al chromite deposits are dominated by Cpx-poor harzburgites. In contrast, those hosting high-Cr chromite deposits have both Cpx-rich and Cpx-poor harzburgites. It is noteworthy that blocks that host high-Cr chromite deposits are often found to have high-Al chromite orebodies. References cited for each ophiolitic block can be found in the Supplementary Information.

Pacific arcs, e.g. Izu–Bonin–Mariana arc (IBM), supporting their subduction initiation origin[6–8]. Studies of the IBM lavas indicate a scenario of gradually weakening asthenospheric upwelling, intensified depletion of magma sources, and strengthening slab dehydration below spreading proto-forearcs in the context of slab rollback, accounting for the eruption of lavas varying from early MORB-like forearc basalts (FAB) to later low-Ti tholeiitic (also called depleted FAB, depleted tholeiitic, and etc.) and boninitic lavas in nascent subduction zones[6,9,10]. Despite the assumed linkages of high-Al and high-Cr chromitites to MORB-like and boninitic-like magmatism, respectively[3,10], recent studies from the mantle perspective revealed that chromite grains in high-Al chromitites, usually featured by low TiO_2 contents, are unlikely the products of typical MORB-like magmatism[11,12], and high-Cr chromitites were more probably generated at a period of flux melting meanwhile with notable asthenospheric upwelling below proto-forearcs[13,14]. This contrasts with the current model of subduction initiation established based on lava compositions alone. Consequently, the genetic relationships among different magmatism, chromite deposits and relevant geodynamic settings during subduction initiation remain to be elaborated, especially from the mantle perspective.

The Zambales ophiolite, located in NW Luzon island of the Philippines (Fig. 2A) has long been recognized to have a subduction initiation origin[15–17]. The Acoje and Coto blocks of the ophiolite are adjacent parts of the same proto-forearc lithosphere with transitional compositions and were generated in an evolving subduction initiation system[12,15,17] (Fig. 2B). Chronological studies show that magmatism in the Coto block took place at 45 Ma, whereas those in the Acoje occurred slightly later (44–43 Ma)[15,18]. The Coto block records magmatism varying from the FAB to low-Ti tholeiitic types with time[15,19], and its Moho transition zone (MTZ) hosts the largest high-Al chromite deposit in the world (6.34 Mt)12 (Fig. 2C and Supplementary Note 1). In contrast, the Acoje block experienced magmatism changing from low-Ti tholeiitic to boninitic ones[17,19], and it hosts a world-class high-Cr chromite deposit (25 Mt) and minor high-Al chromitites along its petrological Moho[14] (Fig. 2D). The mantle sequence of the Coto block comprises mainly Cpx-poor harzburgite (<3 modal% Cpx), and there is no obvious variation of mineral proportions from top to bottom of its mantle sequence[1,12,20] (Fig. 2C), whereas peridotites of the Acoje block vary from Cpx-poor harzburgites with enclosed dunite and Cpx-rich harzburgite (3–5 modal% Cpx) lens at the topmost mantle sequence to Cpx-rich harzburgites and Cpx-poor lherzolites (5–10 modal% Cpx; hereinafter grouped as Cpx-rich harzburgites) at the bottom mantle sequence[1,11,14,20] (Fig. 2D). Minerals in the Cpx-rich harzburgites have compositions overall comparable to those in abyssal peridotites (Fig. 3). The Cpx-poor harzburgites and dunites in the mantle sequences of both blocks were modified from less depleted peridotites by interaction with Mg-rich melts (e.g, parental magmas of chromitites) under increasing melt/rock ratio conditions[11,14] (Supplementary Fig. 1 and Note 1). The differences between the two blocks provide an excellent opportunity for studying the origin of various chromitites and their relationships to diverse magmatism during subduction initiation.

By using numerical calculation and Re–Os isotopes of chromitites and peridotites from the Zambales ophiolite and other representative ophiolites in the world, this study first explores how the parental magmas of different chromitites were formed, from the aspects of both mantle source compositions and requisite degrees of melting, and then restores the chemo–thermal variations of the proto-forearc mantle that resulted from changing geodynamic processes. By integrating all available information, we propose a detailed model for the evolution of subduction initiation and explicate how diverse chromite mineralization and related varying lithological associations arise in ophiolites.

Results and discussion

Mantle fertility during different periods of chromite mineralization

Mantle-derived magmas generally have <4000 ppm Cr, but the Cr_2O_3 contents of chromitites reach dozens of wt%[12]. Such contrasting Cr contents suggest that the volumes of the parental magmas of chromitites must be dozens to hundreds of times larger than those of the chromitites themselves[21]. Therefore, ophiolitic chromitites are commonly thought to be generated via the accumulation of chromite and olivine under magma-dominated environments, e.g. in melt channels or magma chambers[21,22], and their compositions are primarily governed by those of their parental magmas, which are in turn controlled by the nature of the source regions and partial melting degrees. Accordingly, to gain insight into the varying chromite mineralization in

https://doi.org/10.1038/s41467-024-53508-7

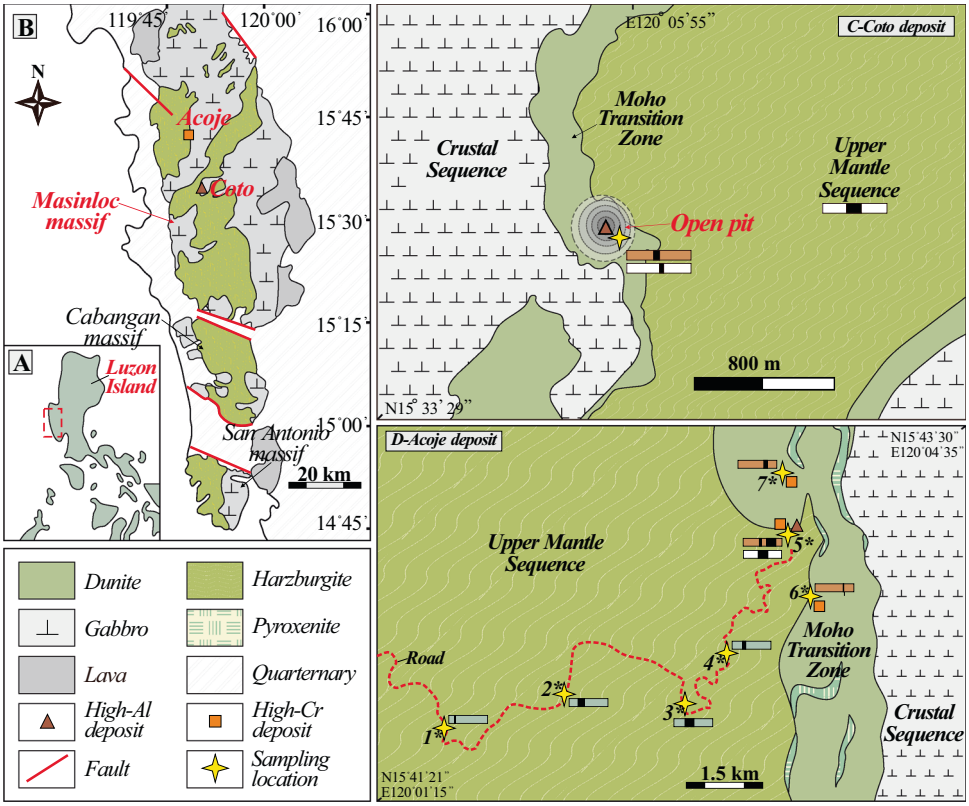

Fig. 2 | Geological maps of the Zambales ophiolite and the Coto and Acoje blocks. A Location of the Zambales ophiolite in the Philippines. **B** Geological map of the Zambales ophiolite and its subdivisions. **C** Geological map of the Coto mining area. **D** Geological map of the Acoje block. The sampling location 5 in the panel D is a mixture area of various rocks, including high-Al chromitites (minor), high-Cr chromitites (minor), dunites (major), Cpx-poor harzburgites (major), and Cpx-rich harzburgites (minor)[11]. The grey, white and brown bars shown near the sampling locations in panels **C**, **D** represent lithologies of Cpx-rich harzburgite, Cpx-poor harzburgite and chromite, respectively. The Cr# of chromite in these rocks can be generally known based on the locations of black bands in the bars, each assumed to have a Cr# range from 0 to 100. Chromite grains in Acoje harzburgites have a large Cr# range, increasing from ~17 at the bottom to ~68 at the top of the mantle sequence. In contrast, chromite grains in the peridotites of the Coto block show a narrow range of Cr#.

ophiolites, the fundamental steps are to estimate the parental magma compositions of different chromitites, mantle source compositions of the parental magmas, and also melting degrees required in the mantle sources. Apart from being controlled by their parental magmas, the compositions of chromite in chromitites can also be affected by subsolidus ionic exchange with olivine, which transfers divalent cations between the two phases[23]. Compared with divalent cations, those of high valence states, e.g. Cr^{3+}, Al^{3+}, and Ti^{4+}, are not easily mobilized[24]. Therefore, they can be used more effectively for evaluating the primary natures and origins of the parental magmas of chromitites.

Overall, chromite grains in the high-Cr chromitites have relatively homogeneous compositions (e.g. Cr# ~ 73 wt%; TiO_2 ~ 0.20 wt%; Fig. 4A), but those in the high-Al chromitites vary in both Cr# and TiO_2, dividing them into Ti-poor and Ti-rich varieties (boundary values defined as 0.10 wt% TiO_2) (Fig. 4A). The TiO_2 contents of melt inclusions in lavas-hosted chromite were found to show good correlation with those of the chromite hosts[24], and regression formulae have been established for estimating the TiO_2 contents of parental magmas of chromitites by using the TiO_2 contents of chromite grains in chromitites[25] (Fig. 4B).

$$TiO_2(Melt) = 1.5907^{*}[TiO_2(high-Al\ Chr)]^{0.6322} \quad (1)$$

$$TiO_2(Melt) = 1.0963^{*}[TiO_2(high-Cr\ Chr)]^{0.7863} \quad (2)$$

Our calculated results suggest that the parental magmas of our high-Cr chromitites have ~0.2–0.4 wt% TiO_2, and those of the Ti-poor and Ti-rich high-Al chromitites have ~0.2–0.4 wt% and 0.5–0.7 wt% TiO_2, respectively. Combined with Cr# of chromite, the parental magmas of high-Cr chromitites have boninitic affinity[17,26] (<0.5 wt% TiO_2; Fig. 4B), consistent with previous findings[3]. However, the parental magmas of high-Al chromitites are found not as traditionally thought akin to typical MORB-like ones (mostly > 0.8 wt% TiO_2), but show obvious affinities with more depleted low-Ti tholeiitic magmas (0.2–0.8 wt% TiO_2; Fig. 4B and references therein).

Ti is an incompatible element in mantle peridotites, and the TiO_2 contents of mantle-derived magmas theoretically decrease either with increasing partial melting degree at a fixed level of mantle fertility or with decreasing mantle fertility at a fixed degree of melting[27] (Fig. 4C). On one hand, PGE studies revealed that the parental magmas of high-Al and high-Cr chromitites were formed by melting of peridotites under relatively low (S-saturated) and high (S-undersaturated) degrees, respectively, regardless of under hydrous condition or not[3,5]. On the other hand, the composition of the proto-forearc mantle is usually considered not as fixed but rather becoming more and more depleted with the progress of subduction initiation[6,7]. Further given that high-Al chromitites were formed earlier than high-Cr chromitites in the framework of subduction initiation, the parental magmas of high-Al chromitites are expected to have more TiO_2 than those of high-Cr chromitites. From the Zambales high-Al chromitites to high-Cr chromitites, however, chromite grains overall show increasing TiO_2 contents (from ~0.03 wt% to 0.28 wt%; Fig. 4A), a feature that can also be seen for ophiolitic chromitites from worldwide (Supplementary Fig. 2A). More surprisingly, the parental magmas of some Ti-poor high-Al chromitites have even less TiO_2 than those of the high-Cr chromitites (Fig. 4A, B). Such results are inconsistent with the combined

https://doi.org/10.1038/s41467-024-53508-7

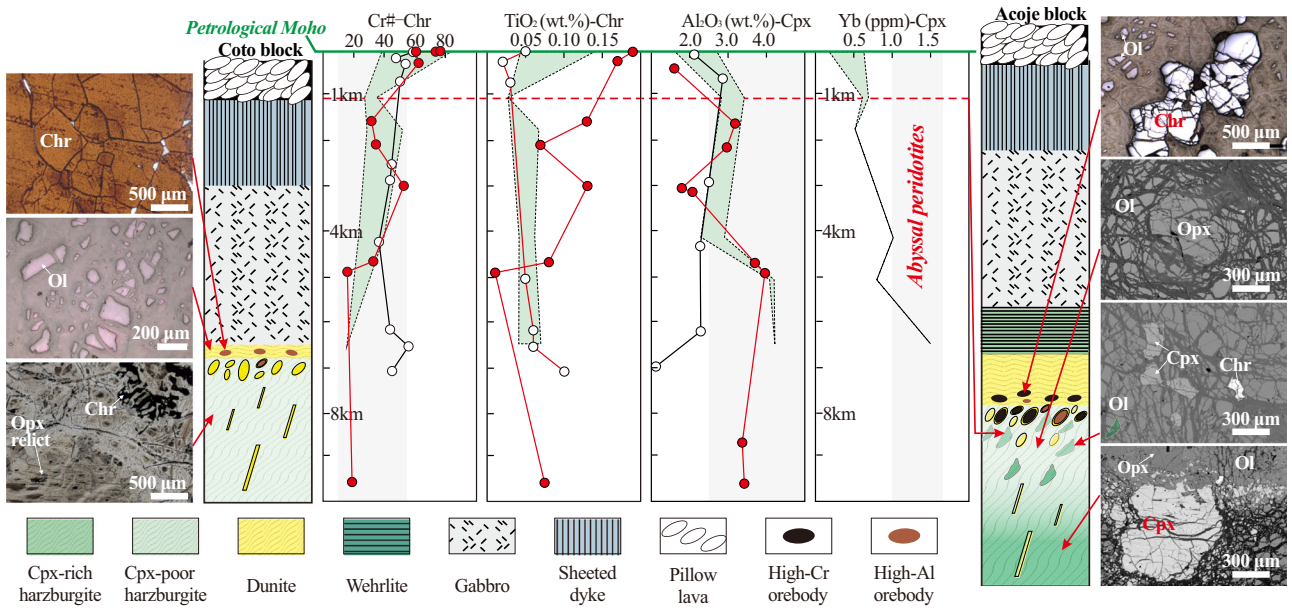

Fig. 3 | Lithological columns of the Coto and Acoje blocks and compositional variations of chromite and clinopyroxene in peridotites at different stratigraphic depths in their mantle sequences. The three photo-micrographs for the Coto blocks show chromitites, dunites, and Cpx-poor harzburgites from top to bottom[12]. The four photo-micrographs for the Acoje block show chromitites, Cpx-poor harzburgites, Cpx-rich harzburgites, and lherzolites[11,14]. The depth of 0 km in the columns marks the locations of petrological Moho. The red and white dots used in the first three columns show the compositions of chromite and clinopyroxene from the mantle rocks of the Acoje and Coto blocks, respectively, with the data from Evans and Hawkins show[20]. The green zones in the columns show the compositional ranges of chromite and clinopyroxene from the Acoje mantle sequence, with relevant data from Zhang et al. show[11,14]. The compositional variations shown in the green zones at a certain depth reflect the variation of lithologies at that stratigraphic level, which resulted from reactions between Mg-rich melts and Cpx-rich harzburgites under varying melt/rock ratio conditions (Supplementary Fig. 1). The ranges of chromite and clinopyroxene compositions from the abyssal peridotites (grey zones) are displayed for comparison. The dashed red line in the composition columns marks a special level featured by the presence of Cpx-rich harzburgites in the background of Cpx-poor harzburgites at the upper part of the Acoje mantle sequence. Detailed lithological distributions in mantle sequences of the two blocks can be found in Supplementary Note 1 and Fig. 2C, D.

effects of higher degrees of melting and more depleted mantle sources as traditionally assumed for high-Cr chromitites compared with high-Al ones.

Comparing the calculated TiO_2 contents for parental magmas of different types of chromitites via the regression formulae and multi-stage fractional melting model (Fig. 4D and Supplementary Note 2), it appears that parental magmas of the high-Cr chromitites were generated via ~15–25% flux melting of moderately depleted mantle sources that had compositions equivalent to ~5–10% melting residues of fertile MORB mantle (FMM) (Fig. 4D). The parental magmas of the Ti-rich high-Al chromitites from both blocks originated from sources with similar compositions to the high-Cr ones but were generated via further 5–15% flux melting. However, parental magmas of the Ti-poor high-Al chromitites were formed by 5–15% flux melting of mantle sources that had compositions equivalent to 10–20% melt residues from the FMM (Fig. 4D). The results above indicate that the parental magmas of all our chromitites were derived from more depleted sources than the FMM, moreso for the Ti-poor high-Al chromitites. Although the formation sequence of Ti-rich and Ti-poor high-Al chromitites in the Coto block needs to be further clarified in a specific geological context, the Zambales proto-forearc mantle had surely become increasingly fertile as the mineralization proceeded from the Ti-poor high-Al chromitites in the early Coto block to the Ti-rich high-Al chromitites and high-Cr chromitites in the younger Acoje block, regardless if the Ti-rich high-Al chromitites in Coto block formed earlier or than the Ti-poor ones. Such a result differs from the conventional view that the mantle sources of magmas simply become more and more depleted with subduction initiation going on[6,7,9], but is consistent with the fact that the mantle sequence of the Acoje block has Cpx-rich harzburgites throughout and shows higher fertility than that of the Coto block (Figs. 2C, D and 3), suggesting fertilization processes in the proto-forearc mantle before the high-Cr mineralization.

Origin of radiogenic Os isotopic ratios of the chromitites

Chromitites from the Zambales ophiolite have large Os isotopic variation, with the high-Al chromitites overall having higher $^{187}Os/^{188}Os$ ratios than the high-Cr ones (0.130–0.150 vs 0.125–0.130) (Fig. 5A–C). This isotopic variation implies either that the varied values are decay products of similar initial Os isotopic compositions under conditions of different Re/Os ratios or that they were initially different from each other. All the chromitites overall have low Re/Os ratios (between 0.001 and 1) and were formed at ~45–43 Ma[15,18] (Fig. 5B). Compared with the significant long half-life of ^{187}Re ($^{187}Re \rightarrow {}^{187}Os$, ~4.3 Gyrs), the Os isotopic systems of the chromitites could not have changed too much after the mineralization, and there should be no difference between the original and current $^{187}Os/^{188}Os$ ratios of the chromitites. Therefore, the contrasting Os isotopic ratios of the high-Al and high-Cr chromitites could not have resulted from the decay of Re, but rather the high-Al chromitites had higher $^{187}Os/^{188}Os$ ratios than the high-Cr ones from the moments of their formation.

The Os budgets of ophiolitic chromitites are not only controlled by their parental magmas but may also be affected by peridotites that had ever reacted with the parental magmas, e.g. during their upward migration[5,28]. Conventionally, chromitites formed in melt-dominated environments, and high-Cr chromitites always have higher Os concentrations than high-Al ones and peridotites[5,29] (Fig. 5D and Supplementary Fig. 2B). Based on the concept of mass balance, the Os budgets of high-Cr chromitites must be less affected by peridotites than those high-Al ones, if any influence existed. Further given that harzburgites from both the Coto and Acoje blocks have indistinguishable Os isotopic ratios (Fig. 5A), the decreasing $^{187}Os/^{188}Os$

https://doi.org/10.1038/s41467-024-53508-7

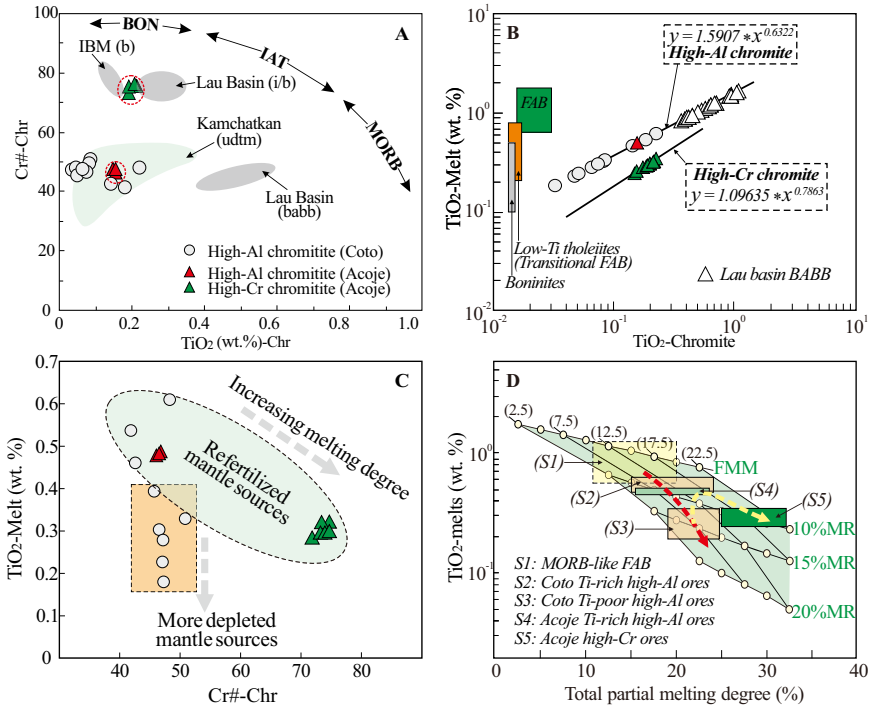

Fig. 4 | Compositions of chromite grains in harzburgites and chromitites and calculated parameters for the parental magmas of chromitites. A Cr# vs TiO_2 of chromite in chromitites and lavas from various backgrounds. BON and b boninite, IAT and i island arc tholeiite, babb back-arc basin basalt, udtm ultra-depleted tholeiitic melt. The diagram was modified after Pearce et al. show[27] and Zhang et al. show[12]. **B** Calculated TiO_2 contents in the parental magmas of chromitites. The equations are from Rollinson et al. show[25]. The TiO_2 ranges of FAB (MORB-like tholeiites)[9], low-Ti tholeiites (depleted FAB)[10,63,64] and boninites[17,26] and the data of chromite from the Lau Basin BABB[70] (depleted types) are also plotted for comparison. **C** Variation of TiO_2 contents in the parental magmas of chromitites with Cr# of chromite in the chromitites. **D** Partial melting degrees are required for the formation of the parental magmas of chromitites. The network in light green colour was drawn based on the modelling results of a series of fractional melting. The four initial mantle sources used for the modelling are FMM and residues (MR) of FMM after 10%, 15%, and 20% melting, respectively. Five melting degrees, 2.5%, 7.5%, 17.5%, 22.5%, and 27.5%, are used during modelling for the selected four mantle sources. Generally, FAB was assumed as the melting products at total degrees of 10–20%, parental magmas of high-Al chromitites and high-Cr chromitites at total degrees below and over 25%, respectively. Details of multi-stage melting accounting for the formation of FAB and parental magmas of different chromitites, e.g. the compositions of their sources and required melting degrees at each stage, can be evaluated based on their TiO_2 contents and required total melting degrees. The transparent yellow rectangle was drawn based on the TiO_2 contents of MORB-like rocks from the Zambales ophiolites[15], and only the TiO_2 contents of those with high MgO, Ni and Cr contents were used. The red and yellow dashed lines represent the evolving fertility in the parental magma sources of FAB and different chromitites (S1–S5). The parameters and equations used for the calculations above can be found in Supplementary Note 2.

trend from the high-Al chromitites to high-Cr ones could not have been caused by involvement of Os from the harzburgites but was primarily controlled by the natures of their parental magmas[30], which in turn reflect different Os isotopic features of the magma sources.

High-Al chromitites from both the Coto and Acoje blocks display radiogenic $^{187}Os/^{188}Os$ ratios at times (Fig. 5A, B). Such a feature is also found for some high-Al chromitites from other ophiolites (Fig. 6), requiring the addition of exotic components to their parental magma sources. Asthenospheric upwelling and slab dehydration are the two dominant processes during subduction initiation[6,7], modifying the compositions of the mantle wedge below proto-forearcs. Asthenosphere underwent Re depletion during crust-mantle differentiation and has lower $^{187}Os/^{188}Os$ ratios than the primitive upper mantle (PUM) (Fig. 5A)[31–33]. As a result, the radiogenic Os isotopic features of the high-Al chromitites could not have resulted from modification by asthenospheric upwelling in their mantle sources. In contrast, the seawater-altered oceanic crust has obviously a higher $^{187}Os/^{188}Os$ ratio than the primitive mantle and is a potential source of the required radiogenic Os[34]. According to experimental studies, Os becomes increasingly mobile in fluids with increasing halogen content and oxygen fugacity[35,36], and can be delivered into the overriding mantle wedges from the subducted slabs at certain depths[34,37]. As a result, the radiogenic Os components in mantle sources of the high-Al chromitites were possibly derived from sinking slabs during subduction initiation.

Effects of refertilization on Os isotopes of the proto-forearc mantle

Because the Os isotopic compositions of all the Zambales chromitites could not have been notably changed by radioactive decay in 45 Ma, the apparently different $^{187}Os/^{188}Os$ ratios of the high-Al and high-Cr chromitites suggest a period of drastic Os isotopic shift in the mantle sources by other means, which decreased the effects of slab components in the proto-forearc mantle from formation of high-Al chromitites to high-Cr ones. Previous studies revealed that melt infiltration may result in the dissolution and re-precipitation of Os-bearing minerals in peridotites[38–40], potentially modifying the Os isotopic systems of peridotites and accounting for the isotopic shift. However, the parental magma sources of all the chromitites, situated stratigraphically deeper than the preserved mantle sequences of the ophiolite, had been lost during tectonic emplacement, making it impossible to observe what happened in the magma sources directly. Even so, modification of the bulk Os isotopic systems of peridotites in the lost mantle sources could be simplified in the way of binary mixing as if in black boxes, and the final $^{187}Os/^{188}Os$ ratios of the modified mantle should be intermediate between their original ratios and those of the reactant melts, however complex the modification processes were. As a result, the addition of low-$^{187}Os/^{188}Os$ components would be the only way of lowering the $^{187}Os/^{188}Os$ ratios of the proto-forearc mantle.

https://doi.org/10.1038/s41467-024-53508-7

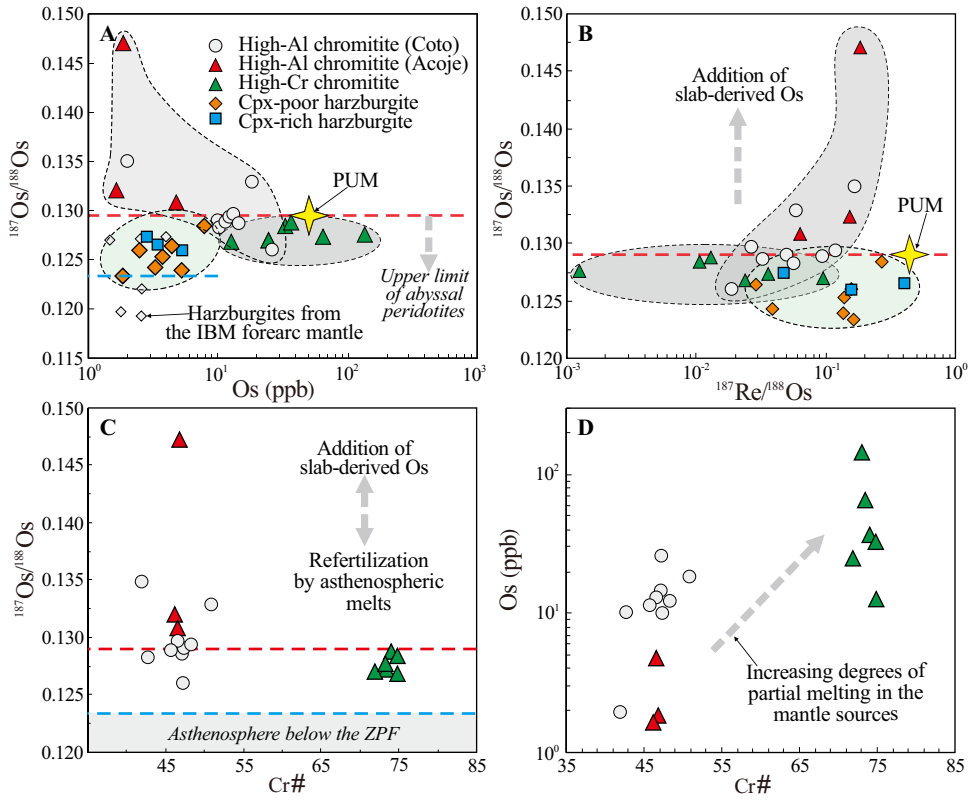

Fig. 5 | Os concentrations and isotopic compositions of different lithologies. **A** Plot of $^{187}Os/^{188}Os$ ratios vs Os concentrations of the chromitites and peridotites. **B** Plot of $^{187}Os/^{188}Os$ vs $^{187}Re/^{188}Os$ ratios of the chromitites and peridotites. **C** Plot of $^{187}Os/^{188}Os$ ratios vs Cr# of chromite grains from the chromitites. **D** Plot of Os concentrations vs Cr# of chromite grains from the chromitites. The red and blue dashed lines in the diagrams denote the upper $^{187}Os/^{188}Os$ limits for abyssal peridotites and the local asthenosphere below the Eocene Zambales proto-forearc, respectively.

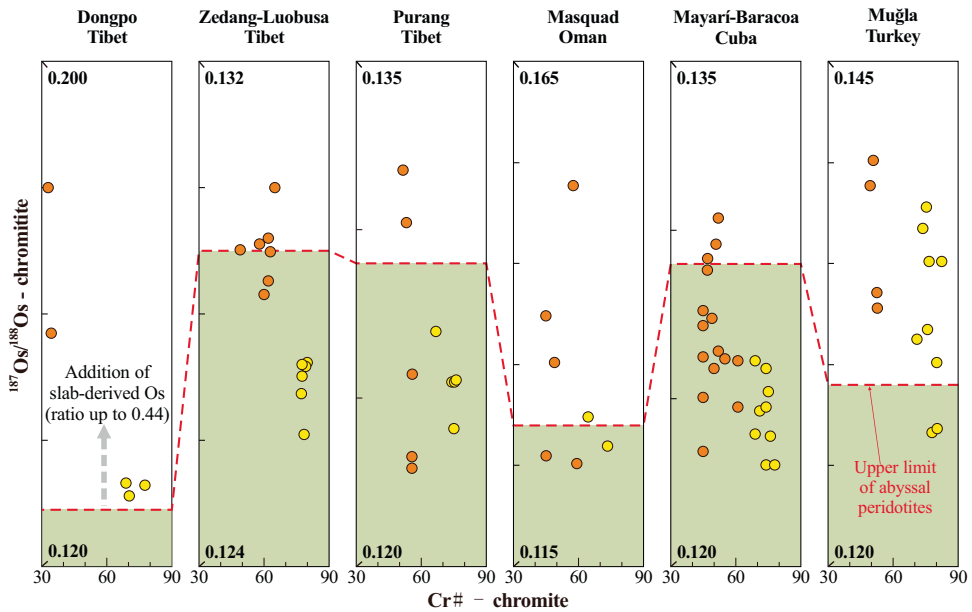

Fig. 6 | Compiled Os isotopic data of concomitant high-Al (brown dots) and high-Cr chromitites (yellow dots) reported for other ophiolites worldwide. The cases of Dongbo[65], Zedang–Luobusa[66,67], Purang[68], Masquad[67], Mayarí-Baracoa[69], and Muğla[4] ophiolites are used. The dashed red line defines the upper $^{187}Os/^{188}Os$ limit for global abyssal peridotites. A decreasing trend of $^{187}Os/^{188}Os$ isotopic ratio can be seen from the high-Al chromitites to high-Cr chromitites in each studied ophiolite. Please note that the Cr#s of chromite from some Zedang–Luobusa chromitites are slightly higher than 60, but such samples are plotted closer to the data points of high-Al chromitites and than to those of the high-Cr ones, indicating their higher affinity to the high-Al chromitites[67]. Such chromitites are thus also grouped as the high-Al ones in the diagram.

Compared with slab-derived components, melts derived from the asthenosphere display lower Os isotopic signatures[33,37,41], falling into the range of abyssal peridotites (0.114–0.129)[42]. Peridotites notably modified by asthenospheric melts would thus have lower $^{187}Os/^{188}Os$ ratios similar to abyssal-like values. This can be exemplified by the case that happened in the subcontinental lithospheric mantle (SCLM) of the North China Craton, which had been highly refertilized by asthenospheric melts during Mesozoic and Cenozoic and transformed to have abyssal-like Os isotopic ratios[43]. On one hand, Cpx-rich harzburgites of the Acoje block also have abyssal-like $^{187}Os/^{188}Os$ ratios (0.1267–0.1288; Fig. 5A, B). On the other hand, clinopyroxene grains in the Cpx-rich harzburgites show signs of melt impregnation and even make up diopsidite veins (Fig. 3). Combined with the abyssal-like compositions of clinopyroxene and chromite in the Cpx-rich harzburgites, such moderately depleted harzburgites cannot be residues of low to moderate degrees of melting but were refertilized products of previous Cpx-poor harzburgites (CP-Hz I, not those in the current Acoje mantle sequence) by asthenospheric melts, which imposed higher Al_2O_3 contents and abyssal-like REE compositions on clinopyroxene and lowered the Cr#s of chromite to even <20[1,14,20] (Fig. 3). Consequently, the decreasing $^{187}Os/^{188}Os$ ratios from the high-Al chromitites to high-Cr ones can be best explained by modification of asthenospheric melts. Moreover, such a postulation corroborates that the lost parental magma sources of the high-Cr chromitites were refertilized, as did in the preserved mantle sequence of the Acoje block, also consistent with the result postulated based on the TiO_2 contents of chromite. As a result, the Os isotopic variations of the chromitites depict a scenario of enhancing the contribution of asthenosphere but waning slab impact [$Os_{slab}/(Os_{slab} + Os_{asthenosphere})$ rather than Os_{slab} itself] in the proto-forearc mantle prior to the high-Cr chromite mineralization.

Although the Os isotopic ratios of many chromitites fall into the general range of abyssal peridotites, the values are overall higher than those of peridotites in the mantle sequences. Generally, mantle harzburgites result from either partial melting of lherzolites or modification of lherzolites by Mg-rich melts[44,45]. In the uppermost Acoje mantle sequence, Cpx-rich harzburgite bodies occur as an enclosed lens in the Cpx-poor harzburgites at places, and chromite grains show positively correlated TiO_2 and Cr# from the Cpx-rich to Cpx-poor harzburgites, a trend consistent with the result of melt-peridotite reaction but contradictory to that of mantle melting[27] (Fig. 3). These features suggest that the Cpx-rich harzburgites, refertilized products of the early CP-Hz I, later reacted with Mg-rich magmas and formed new Cpx-poor harzburgites (CP-Hz II; Fig. 3 and Supplementary Note 1). On one hand, the higher $^{187}Os/^{188}Os$ ratios of all the chromitites mean that reaction with their parental magmas would impose more radiogenic Os features on the harzburgites. On the other hand, Os isotopes are commonly thought not to fractionate during partial melting, and harzburgites formed via partial melting of lherzolites should have comparable Os isotopic compositions to the lherzolitic proto-liths. Given that the origins of all harzburgites in ophiolitic mantle sequences can be initially traced back to decompressional melting of the asthenosphere, despite their refertilization and Mg-rich melt modification histories, the local asthenosphere below the Zambales proto-forearc should have $^{187}Os/^{188}Os$ ratio in any cases no more than our harzburgites, which are mostly below 0.1275 (Fig. 5A–C). Subsequently, the more radiogenic Os isotopic features of the chromitites than the harzburgite indicate that the refertilization only lowered $^{187}Os/^{188}Os$ ratios of the previously hydrated Zambales proto-forearc mantle but did not completely eliminate the impact of slab components. Slab-derived Os actually still existed in the parental magma sources of all chromitites, regardless if their $^{187}Os/^{188}Os$ ratios were abyssal-like or not.

Temperature variation during different types of chromite mineralization

Generally, bulk-rock fertility, fluid content and geothermal gradient affect the partial melting degree of peridotites[46]. Although the mantle sources of our Ti-rich high-Al chromitites share similar fertility to those of the high-Cr ones based on the TiO_2-related calculation, the more radiogenic Os isotopic features of the high-Al chromitites suggest stronger impact of slab fluids in their mantle sources than in those of the high-Cr ones. Given that the solidus temperature of peridotites can be effectively decreased by the addition of fluids, higher degrees of melting are more likely to occur in mantle sources of the high-Al chromitites than in those of the high-Cr ones under the same geothermal gradients. This is contrary to the view that the degree of mantle melting required for the formation of high-Al chromitites is lower than that for the formation of high-Cr chromitites[3,5]. The logical explanation would be that the high-Al chromitites formed at lower geothermal gradient conditions than the high-Cr ones, and there was a period of heating between their respective generation.

Chromite and olivine are both nominally anhydrous phases. The water contents in the parental magma sources of chromitites are thus difficult to determine, making it impossible to constrain the formation temperatures of the parental magmas precisely. In spite of different geothermometers developed, the calculated values merely define the equilibrium temperatures for inter-mineral elemental exchange under subsolidus conditions, far below the crystallization temperatures of chromite and olivine, not to mention to be compared with the formation temperatures of their parental magmas. To better understand this issue, experimental work and melt inclusion studies provide possible windows (Fig. 7A, B). Experimental studies show that melts that equilibrate with high-Al chromite are generated under lower temperature conditions than those equilibrating with high-Cr chromite, regardless of the mantle source compositions[47,48] (Fig. 7B). Melt inclusions in chromite grains are generally interpreted as trapped parental melts of the chromite hosts. Given that chromite is the first crystallized phase from the parental magmas of chromitites[3,21], the homogenization temperatures of melt inclusions in chromite from chromitites could be approximately taken as the liquidus temperatures of their parental magmas[49]. According to previous studies, the melt inclusions in high-Al chromite can be homogenized completely at ~1300 °C[50,51], whereas those in high-Cr chromite and associated olivine phenocrysts from picritic and boninites generally require higher homogenization temperatures, even up to 1400 °C[49,52] (Fig. 7B). Consequently, both experimental and melt inclusion studies suggest the parental magmas of high-Cr chromitites generally formed under higher temperature conditions than those of high-Al ones, also supporting the presence of a heating period from the formation of high-Al chromitites to that of high-Cr ones in ophiolites.

Origins of different types of chromite deposits

Our results show that the parental magmas of high-Al chromitites in the Coto block originated from mantle sources that were chemically equivalent to ~10–20% melting residues of the FMM. This earlier 10–20% melting event was possibly linked to the extraction of MORB-like FAB magmas from the FMM (asthenosphere) below the Zambales proto-forearc, which happened at the beginning of subduction initiation in the region (S1 in Fig. 4D and Fig. 8A), present as lavas and dykes in the Coto block[15]. Although high-Al chromitites have long been taken as products of MORB-like magmatism[3], our studies do not support such an argument, probably because the residual mantle left after production of MORB-like magmas still contains clinopyroxene and chromite, both of which retain Cr during partial melting and limit the concentrations of Cr in magmas below its oversaturation level (~1450 ppm)[53]. This is supported by the fact that melt inclusions captured in MORB-hosted olivine phenocrysts, which crystallized the earliest from magmas, generally have <700 ppm Cr[54], suggesting that

https://doi.org/10.1038/s41467-024-53508-7

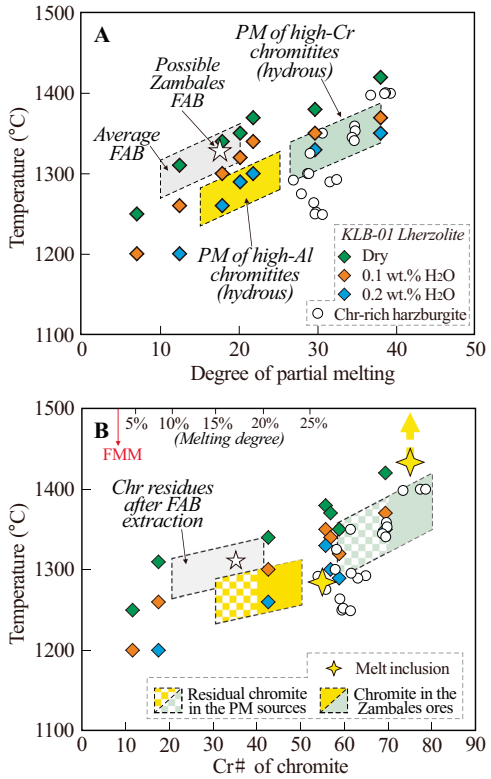

Fig. 7 | Complied temperature data regarding the formation of chromite with varying Cr#. A Variation of partial melting temperature with a partial melting degree for different peridotites. The data of diamonds and dots are from the experimental work on lherzolite[47] and harzburgite[48], respectively. The grey, yellow and green areas in the panel define the formation temperatures of FAB, parental magmas of high-Al chromitites and parental magmas of high-Cr chromitites, based on the assumptions that the total melting degrees required for their formation are 10–20% (nearly anhydrous), 15–25% (hydrous), and >25% (hydrous), respectively. **B** Variation of partial melting temperature with Cr# of chromite in peridotites. The data of yellow stars in the panel show the crystallization temperature of natural high-Al and high-Cr chromite grains based on melt inclusion studies[49,51]. Because chromite grains crystallized from a certain batch of melt at lower pressure are found to have higher Cr# than those crystallized at higher pressures, those residual chromite in the parental magma (PM) sources of chromitites theoretically had lower Cr# than the chromite in chromitites that formed at shallower levels, and the parental magmas of chromitites should be formed at lower temperature conditions than those ranges defined by the Cr# of chromite in chromitites, which can be read from the grided and solid parts in the parallelograms, respectively (yellow for high-Al chromitites, green for high-Cr chromitites). The Cr# range of chromite for the FAB in panel B was determined based on that the Cr# of chromite residues is found to be 20–40 when the melting degree ranges from 10% to 20%[47]. The white quadrangular stars in the panels mark the location of postulated chromite in the residual mantle sources of Zambales FAB, which were likely generated by melting of FMM at total degrees of 15–20% based on the calculations (Fig. 4D).

typical MORB-like magmas do not have enough Cr for the oversaturation of chromite.

After extraction of FAB at the earliest stage of proto-forearc spreading during subduction initiation, the uppermost part of the asthenospheric mantle would generally be replaced by harzburgites[6,7,9]. Such harzburgitic mantle had comparatively higher Cr concentrations than the FMM and was prone to yield more Cr-rich melts than MORB-like ones at similar partial melting degrees, facilitating oversaturation of chromite from magmas and formation of chromitites. With harzburgitization of the uppermost mantle below the Zambales proto-forearc, the regional geothermal gradient would be decreased with the deepening of the lithosphere-asthenosphere boundary (LAB) (Fig. 8A, B). This is a similar process to the decrease in geothermal gradient in SCLM with the thickening of SCLM roots during cratonization[55,56]. Harzburgitization would also elevate the solidus temperatures of peridotites and make further melting difficult. The combined effects of harzburgitization and lowered geothermal gradient mean that decreasing the solidus temperature of the mantle by fluids was particularly necessary in order to initiate further partial melting in the Zambales proto-forearc mantle. This not only explains why some high-Al chromitites show remarkably radiogenic Os isotopic features, but also suggests that noticeable slab dehydration and flux melting had already started at the stage of post-FAB tholeiitic magmatism, much earlier than the development of boninitic magmatism.

Although high-Al chromitites, especially the Ti-rich variety, are found in both the Coto and Acoje blocks, their associated peridotites differ from each other. The whole mantle sequence of the Coto block is dominated by Cpx-poor harzburgites, but high-Al chromitites in the Acoje block are hosted in a mixed zone of both Cpx-poor and Cpx-rich harzburgites. These differences suggest that high-Al chromitites in the two blocks are unlikely to form at the same evolutionary stage of subduction initiation, as was also supported by the different ages of the two blocks. Considering that the formation of the Cpx-rich harzburgites in the Acoje block resulted from the refertilization of more depleted harzburgites by asthenospheric melts[14], the Ti-rich high-Al chromitites in the Acoje block are best explained to have been formed no earlier than the refertilization. According to melting-related calculations, the parental magma sources of the Ti-rich high-Al chromitites and Ti-poor ones had moderately depleted and highly depleted compositions, respectively (Fig. 4D). Since no evidence supports that the mantle sequence of the Coto block had been refertilized, the Ti-rich high-Al chromitites in the Coto block must have formed earlier than the Ti-poor ones. This is because a reversal formation order of the two types of high-Al chromitites would require a similar refertilization process in the Coto block as in the Acoje block, producing new Cpx-rich harzburgites and restoring Ti content in the Coto mantle sequence. As such, variation of high-Al chromitites from the Ti-rich to Ti-poor varieties in the Coto block probably reflects increasingly depleted magma sources (S2–S3 in Fig. 4D). Because the parental magmas of the Coto Ti-rich high-Al chromitites have compositions close to the most depleted FAB magmas found in the block (S2 in Fig. 4D), it is reasonable to position the formation of these Ti-rich high-Al chromitites at final stage of the FAB magmatism or immediately after the FAB magmatism in the Zambales proto-forearc, so the moderately depleted compositions required for the parental magma sources of such high-Al chromitites could be ensured (Fig. 8A). Similar to the Coto block, the compositional variation of high-Al chromitites in other ophiolites that contain only high-Al chromite deposits and lack Cpx-rich harzburgites in their mantle sequences can be explained in the same way (Fig. 1).

Although the decreasing mantle fertility and intensified slab dehydration found from the FAB magmatism to high-Al chromite mineralization in the Coto block is consistent with the current model of subduction initiation, the Zambales proto-forearc mantle manifested increasing contribution of asthenospheric components but waning slab impact from the mineralization stage of high-Al chromitites to that of high-Cr ones, indicative of a new period of notable asthenospheric upwelling in the context of enhanced slab rollback before the high-Cr chromite mineralization (Fig. 8B–D), which has not been mentioned yet in the current evolutionary model subduction initiation. Definitely, the re-upwelling process of the asthenosphere not only replenished fertile components (e.g. Ca, Al, and Ti) in the overlying hydrated mantle and refertilized the mantle into Cpx-rich harzburgites, but also elevated the geothermal gradient in the mantle, facilitating productions of the parental magmas of early Ti-rich high-Al chromitites and later high-Cr ones under increasing temperature conditions (Fig. 8B–D and S3–S4 in Fig. 4D). Although the refertilization probably started prior to the formation of all Acoje chromitites,

https://doi.org/10.1038/s41467-024-53508-7

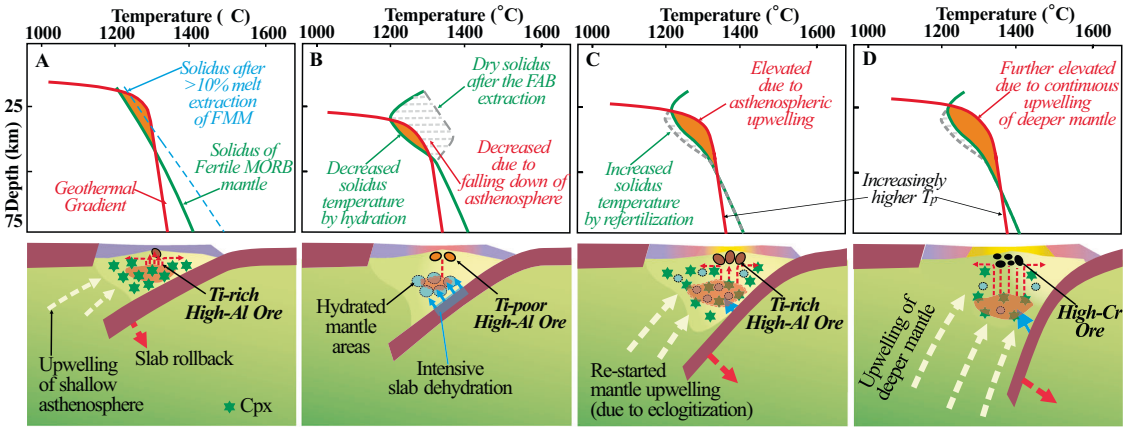

Fig. 8 | Phase diagrams and cartoons showing the mineralization conditions of different types of chromitites in the Zambales proto-forearc mantle. A Initial slab rollback during subduction initiation caused an upwelling of the asthenosphere (in green) into the mantle wedge and formed FAB and Cpx-poor harzburgitic residues (in yellow). Ti-rich high-Al chromitites can theoretically be formed during the stage of depleted FAB magmatism. **B** Exaction of FAB magmas and harzburgitization in the mantle wedge lowered the lithosphere-asthenosphere boundary (LAB boundary between the yellow and green parts) and geothermal gradient. However, slab dehydration lowered the solidus temperature of the harzburgitic mantle wedge and caused flux melting of the mantle with varying fertility, producing melts and high-Al chromitites with varying Ti contents. **C** Eclogitization of the subsiding slab accelerated the rate of slab rollback, causing a new period of marked asthenospheric upwelling. This caused remarkable asthenospheric upwelling and replenished fertile components into the mantle wedge above, generating Cpx-rich harzburgites and elevating the geothermal gradient. Melts derived from the refertilized but still hydrous mantle were comparatively richer in TiO_2 and formed Ti-rich high-Al chromitites. **D** With slab rollback and asthenospheric upwelling going on, the geothermal gradient was elevated to a high enough level to generate boninitic-like melts, resulting in high-Cr chromitites in the mantle wedge. It is noted that the positions of solidus and geothermal gradients featured in the phase diagrams are used for illustrative purposes only, and they are not strictly constrained given the complex physio–chemical conditions.

the Ti-rich high-Al chromitites still show more radiogenic Os isotopic compositions than the high-Cr chromitites. This suggests that the impact of slab components on the proto-forearc mantle remained very strong and had not yet been largely diluted by the replenished asthenospheric components during the early stage of asthenospheric re-upwelling. Further given the minimal presence of slab fluids in mantle sources of typical FAB[6,9], the slab impact in the proto-forearc mantle was probably the most noticeable during the stage of high-Al chromite mineralization. In spite of the refertilization event, it is highly noted that the parental magmas of all the Acoje chromitites originated from more depleted mantle sources than the FMM (Fig. 4D). This suggests that the fertility of the proto-forearc mantle was not recovered to the level of FMM anymore after the MORB-like FAB magmatism. Accordingly, the extent of asthenospheric upwelling and rate of slab rollback during high-Cr chromite mineralization was not as remarkable as those during the FAB magmatism, even though both processes were accelerated after the period of Ti-poor high-Cr chromite mineralization.

Like the case of the Acoje block, other ophiolitic blocks that host high-Cr chromite deposits also contain a noticeable amount of abyssal-like peridotites (Fig. 1). For those ophiolitic blocks having both high-Al and high-Cr chromitites, high-Al chromitites overall also have more radiogenic Os isotopic compositions than high-Cr ones (Fig. 6). These similarities suggest upwelling of asthenosphere is possibly a prevalent feature before high-Cr chromite mineralization in proto-forearc mantle. Apparently, as long as high-Cr chromitites were finally generated during subduction initiation, an earlier period must have existed when the physio–chemical condition of the mantle satisfied the formation of high-Al chromitites. These suppositions explain why high-Cr chromitites are generally hosted in mantle sequences that are featured by the presence of Cpx-rich harzburgites and high-Al chromitites (Fig. 1).

Geodynamic implication

Based on geological arguments and calculations, the new-round enhanced slab rollback was possibly caused by eclogitization of the sinking slab below the Zambales proto-forearc[57,58], inducing larger density contrast between the sinking slab and surrounding mantle peridotite and accelerating subsidence rate of the slab. Given that slab rollback is the fundamental way of driving asthenospheric upwelling below proto-forearcs, eclogitization of the sinking slab likely induced sustainable ascent of deep asthenospheric materials with higher potential temperatures (Fig. 8D), facilitating higher degrees of mantle melting and generation of more Mg-rich magmas (e.g. boninitic-like ones). In particular, such a geodynamic scenario was proposed by some to account for high-Ca boninitic magmatism[59], supporting the distinctive affinity between high-Cr chromitites and high-Ca boninitic magmas. Comparatively, low-Ca boninitic magmatism, overall happening later than the high-Ca one, is thought to mark the start of real subduction and produced via flux melting of highly refractory harzburgitic mantle[16,60], implying that fertility of the proto-forearc mantle becomes poorer again before the completion of subduction initiation.

Without slab eclogitization happening, the density contrast between sinking slabs and the mantle is generally negligible. Subsidence of slabs under such a circumstance would occur at slow rates, and subduction initiation may not be as sustainable as in the case of eclogitization and may even cease after the mineralization of Ti-poor high-Al chromitites. Accordingly, asthenospheric upwelling, transfer of heat and mantle refertilization would be less effective such that there would be no further high-Cr chromite mineralization, and the formation of high-Al chromitites itself more likely marks a trough period of fertility and geothermal gradient but a climax stage of slab impact in the proto-forearc mantle. Such a deduction explains why the mantle sequences of ophiolites that only host high-Al deposits are generally dominated by Cpx-poor harzburgites (Fig. 1). However, it is noted that the evolutionary pathways of other ophiolites are not always the same as that of the classical Zambales ophiolites, and the varieties of generated chromitites likely differ from one ophiolite to another. For example, in case eclogitization and accelerated rollback of slabs occur soon after the FAB magmatism, upwelling of the asthenosphere would quickly take place above the slab and induce refertilization in the proto-forearc mantle. Accordingly, the high-Al chromitites generated under such a circumstance would possibly be all Ti-rich ones.

Methods

Eighteen chromitites and ten harzburgites from the Acoje and Coto block were selected for Re–Os concentration and isotopic analyses, undertaken at the Guangzhou Institute of Geochemistry, Chinese Academy of Sciences[61]. Chromite grains from the chromitites were first hand-picked and then pulverized. Less than 50 mg of powdered chromite and ~500 mg of powdered harzburgite were weighed and spiked with enriched ^{190}Os and ^{185}Re solutions. These samples were then dissolved using ~10 ml of inverse aqua regia in Carius tubes under constant conditions of 230 °C for 24 h. Os was extracted from the aqua regia with carbon tetrachloride solvent and back-extracted into concentrated HBr acid. Further Os purification was attained by microdistillation with chromic acid. Rhenium was separated and purified from the remaining solutions using anion exchange chromatography with AG1-X8 resin. Samples used in this study were divided into three batches for chemical purification. Each batch had ~10 samples and was accompanied by a reference material BIR-1 and a blank sample for the quality control of resultant data. The Re concentrations were measured with isotope dilution coupled with ICP-MS, the Os concentrations and isotopic ratios with TIMS.

The average Re and Os concentrations of blanks are 1.153 ± 1.934 pg (2 SD, $n = 3$) and 0.784 ± 0.051 pg (2 SD, $n = 3$), respectively. Such values are markedly lower than those of our samples and reference material BIR-1 (>0.027 ppm for Re and >1.659 ppm for Os), indicating insignificant Re and Os contamination during the chemical purification. Reproducibilities of the reference material BIR-1 are 0.79% for Re concentration, 3.00% for Os concentration, 0.06% for ^{187}Os/^{188}Os and 3.68% for ^{187}Re/^{188}Os. The average Re concentration, Os concentration, ^{187}Os/^{188}Os, and ^{187}Re/^{188}Os of the reference material BIR are 0.688 ± 0.017 ppb (2 SD, $n = 3$), 0.337 ± 0.001 ppb (2 SD, $n = 3$), 0.13412 ± 0.00034, and 9.845256 ± 0.248 (2 SD, $n = 3$), respectively (Supplementary Table 1), in good agreement with published results[62] (Re, 0.675 ± 14 ppb; Os, 0.355 ± 0.040 ppb; ^{187}Os/^{188}Os, 0.13372 ± 0.00080; and ^{187}Re/^{188}Os, 9.17 ± 1.00). The 2se values for the ^{187}Os/^{188}Os of our samples are all below 0.00060, confirming the high precision of our data.

Data availability

All data used in this study can be found both in Supplementary Table 1 and from Figshare via https://doi.org/10.6084/m9.figshare.26271721.v1.

Code availability

No code was used in this study.

References

1. Leblanc, M. & Violette, J. F. Distribution of aluminum-rich and chromium-rich chromite pods in ophiolite peridotites. *Econ. Geol.* **78**, 293–301 (1983).
2. González-Jiménez, J. M. et al. Chromitites in ophiolites: How, where, when, why? Part II. The crystallization of chromitites. *Lithos* **189**, 140–158 (2014).
3. Zhou, M. F., Robinson, P. T., Malpas, J. & Li, Z. Podiform chromitites in the Luobusa ophiolite (southern Tibet): implications for melt-rock interaction and chromite segregation in the upper mantle. *J. Petrol.* **37**, 3–21 (1996).
4. Uysal, I. et al. Petrology of Al-and Cr-rich ophiolitic chromitites from the Muğla, SW Turkey: implications from composition of chromite, solid inclusions of platinum-group mineral, silicate, and base-metal mineral, and Os-isotope geochemistry. *Contrib. Mineral. Petrol.* **158**, 659–674 (2009).
5. González-Jiménez, J. M. et al. High-Cr and high-Al chromitites from the Sagua de Tánamo district, Mayarí-Cristal ophiolitic massif (eastern Cuba): constraints on their origin from mineralogy and geochemistry of chromian spinel and platinum-group elements. *Lithos* **125**, 101–121 (2011).
6. Whattam, S. A. & Stern, R. J. The 'subduction initiation rule': a key for linking ophiolites, intra-oceanic forearcs, and subduction initiation. *Contrib. Mineral. Petrol.* **162**, 1031–1045 (2011).
7. Stern, R. J., Reagan, M., Ishizuka, O., Ohara, Y. & Whattam, S. To understand subduction initiation, study forearc crust: to understand forearc crust, study ophiolites. *Lithosphere* **4**, 469–483 (2012).
8. Ishizuka, O., Tani, K. & Reagan, M. K. Izu–Bonin–Mariana forearc crust as a modern ophiolite analogue. *Elements* **10**, 115–120 (2014).
9. Reagan, M. K. et al. Fore-arc basalts and subduction initiation in the Izu–Bonin–Mariana system. *Geochem. Geophy. Geosy.* https://doi.org/10.1029/2009GC002871 (2010).
10. Morishita, T. et al. Diversity of melt conduits in the Izu–Bonin–Mariana forearc mantle: implications for the earliest stage of arc magmatism. *Geology* **39**, 411–414 (2011).
11. Zhang, P. F., Zhou, M. F. & Yumul, G. P. Jr Coexistence of high-Al and high-Cr chromite orebodies in the Acoje block of the Zambales ophiolite, Philippines: evidence for subduction initiation. *Ore Geol. Rev.* **126**, 103739 (2020b).
12. Zhang, P. F. et al. Sluggish slab rollback at the early stage of flux melting during subduction initiation: Li isotopic evidence from the Coto high-Al chromite deposit, Zambales ophiolite, Philippines. *J. Geophys. Res. -Sol. Ea.* **128**, e2022JB025562 (2023).
13. Zhang, P. F. et al. Evolution of nascent mantle wedges during subduction initiation: Li–O isotopic evidence from the Luobusa ophiolite, Tibet. *Geochim. Cosmochim. Acta* **245**, 35–58 (2019).
14. Zhang, P. F., Zhou, M. F., Yumul, G. P. Jr & Wang, C. Y. Geodynamic setting of high-Cr chromite mineralization in nascent subduction zones: Li isotopic and REE constraints from the Zambales ophiolite, Philippines. *Lithos* **384**, 105975 (2021).
15. Geary, E. E., Kay, R. W., Reynolds, J. C. & Kay, S. M. Geochemistry of mafic rocks from the Coto Block, Zambales ophiolite, Philippines: trace element evidence for two stages of crustal growth. *Tectonophysics* **168**, 43–63 (1989).
16. Pearce, J. A. et al. Boninite and harzburgite from Leg 125 (Bonin–Mariana forearc): a case study of magma genesis during the initial stages of subduction. In *Proc The Ocean Drilling Program*, Scientific Results (eds. Fryer, P., Pearce, J.A., Stokking, L.B. et al.) 623–659 (Ocean Drilling Program, College Station, 1992).
17. Perez, A., Umino, S., Yumul, G. P. Jr & Ishizuka, O. Boninite and boninite-series volcanics in northern Zambales ophiolite: doubly vergent subduction initiation along Philippine Sea plate margins. *Solid Earth* **9**, 713–733 (2018).
18. Encarnación, J. P., Mukasa, S. B. & Obille, E. C. Jr Zircon U-Pb geochronology of the Zambales and angat ophiolites, Luzon, Philippines: evidence for an Eocene arc-back arc pair. *J. Geophys. Res. Sol. Ea.* **98**, 19991–20004 (1993).
19. Yumul, G. P. Varying mantle sources of supra-subduction zone ophiolites: REE evidence from the Zambales ophiolite complex, Luzon, Philippines. *Tectonophysics* **262**, 243–262 (1996).
20. Evans, C. & Hawkins, J. W. Jr Compositional heterogeneities in upper mantle peridotites from the Zambales range ophiolite, Luzon, Philippines. *Tectonophysics* **168**, 23–41 (1989).
21. Zhang, P. F. et al. Iron isotopic fractionation and origin of chromitites in the paleo-Moho transition zone of the Kop ophiolite, NE Turkey. *Lithos* **268**, 65–75 (2017).
22. Arai, S. & Yurimoto, H. Podiform chromitites of the Tari–Misaka ultramafic complex, southwestern Japan, as mantle-melt interaction products. *Econ. Geol.* **89**, 1279–1288 (1994).
23. Arai, S. Characterization of spinel peridotites by olivine-spinel compositional relationships: review and interpretation. *Chem. Geol.* **113**, 191–204 (1994).

24. Kamenetsky, V. S., Crawford, A. J. & Meffre, S. Factors controlling chemistry of magmatic spinel: an empirical study of associated olivine, Cr-spinel and melt inclusions from primitive rocks. *J. Petrol.* **42**, 655–671 (2001).
25. Rollinson, H. The geochemistry of mantle chromitites from the northern part of the Oman ophiolite: inferred parental melt compositions. *Contrib. Mineral. Petrol.* **156**, 273–288 (2008).
26. Ishizuka, O., Taylor, R. N., Umino, S. & Kanayama, K. Geochemical evolution of arc and slab following subduction initiation: a record from the Bonin Islands, Japan. *J. Petrol.* **61**, egaa050 (2020).
27. Pearce, J. A., Barker, P. F., Edwards, S. J., Parkinson, I. J. & Leat, P. T. Geochemistry and tectonic significance of peridotites from the south sandwich arc–basin system, South Atlantic. *Contrib. Mineral. Petrol.* **139**, 36–53 (2000).
28. O'Driscoll, B., Walker, R. J., Day, J. M., Ash, R. D. & Daly, J. S. Generations of melt extraction, melt–rock interaction and high-temperature metasomatism preserved in peridotites of the ~497 Ma Leka Ophiolite Complex. *Nor. J. Petrol.* **56**, 1797–1828 (2015).
29. Uysal, İ. et al. Coexistence of abyssal and ultra-depleted SSZ type mantle peridotites in a Neo-Tethyan Ophiolite in SW Turkey: constraints from mineral composition, whole-rock geochemistry (major–trace–REE–PGE), and Re–Os isotope systematics. *Lithos* **132**, 50–69 (2012).
30. O'Driscoll, B. et al. Chemical heterogeneity in the upper mantle recorded by peridotites and chromitites from the Shetland ophiolite complex, Scotland. *Earth Planet Sc. Lett.* **333**, 226–237 (2012).
31. Meisel, T., Walker, R. J., Irving, A. J. & Lorand, J. P. Osmium isotopic compositions of mantle xenoliths: a global perspective. *Geochim. Cosmochim. Acta* **65**, 1311–1323 (2001).
32. Meisel, T., Walker, R. J. & Morgan, J. W. The osmium isotopic composition of the Earth's primitive upper mantle. *Nature* **383**, 517–520 (1996).
33. Walker, R. J., Prichard, H. M., Ishiwatari, A. & Pimentel, M. The osmium isotopic composition of convecting upper mantle deduced from ophiolite chromites. *Geochim. Cosmochim. Acta* **66**, 329–345 (2002).
34. Turner, S., Handler, M., Bindeman, I. & Suzuki, K. New insights into the origin of O–Hf–Os isotope signatures in arc lavas from Tonga–Kermadec. *Chem. Geol.* **266**, 187–193 (2009).
35. Brandon, A. D., Creaser, R. A., Shirey, S. B. & Carlson, R. W. Osmium recycling in subduction zones. *Science* **272**, 861–886 (1996).
36. Xiong, Y. & Wood, S. A. Experimental quantification of hydrothermal solubility of platinum-group elements with special reference to porphyry copper environments. *Miner. Petrol.* **68**, 1–28 (2000).
37. Saha, A. et al. Slab devolatilization and Os and Pb mobility in the mantle wedge of the Kamchatka arc. *Earth Planet Sc. Lett.* **236**, 182–194 (2005).
38. Büchl, A., Brügmann, G., Batanova, V. G., Münker, C. & Hofmann, A. W. Melt percolation monitored by Os isotopes and HSE abundances: a case study from the mantle section of the Troodos ophiolite. *Earth Planet Sc. Lett.* **204**, 385–402 (2002).
39. Büchl, A., Brügmann, G. E., Batanova, V. G. & Hofmann, A. W. Os mobilization during melt percolation: the evolution of Os isotope heterogeneities in the mantle sequence of the Troodos ophiolite, Cyprus. *Geochim. Cosmochim. Acta* **68**, 3397–3408 (2004).
40. Ackerman, L. et al. Effects of melt percolation on highly siderophile elements and Os isotopes in subcontinental lithospheric mantle: a study of the upper mantle profile beneath Central Europe. *Geochim. Cosmochim. Acta* **73**, 2400–2414 (2009).
41. Büchl, A., Brügmann, G. & Batanova, V. G. Formation of podiform chromitite deposits: implications from PGE abundances and Os isotopic compositions of chromites from the Troodos complex, Cyprus. *Chem. Geol.* **208**, 217–232 (2004).
42. Liu, C. Z., Xu, Y. & Wu, F. Y. Limited recycling of crustal osmium in forearc mantle during slab dehydration. *Geology* **46**, 239–242 (2018).
43. Zhang, H. F. et al. Evolution of subcontinental lithospheric mantle beneath eastern China: Re–Os isotopic evidence from mantle xenoliths in Paleozoic kimberlites and Mesozoic basalts. *Contrib. Mineral. Petrol.* **155**, 271–293 (2008).
44. Edwards, S. J. & Malpas, J. Multiple origins for mantle harzburgites: examples from the Lewis Hills, Bay of Islands ophiolite, Newfoundland. *Can. J. Earth Sci.* **32**, 1046–1057 (1995).
45. Kelemen, P. B., Dick, H. J. & Quick, J. E. Formation of harzburgite by pervasive melt/rock reaction in the upper mantle. *Nature* **358**, 635–641 (1992).
46. Hirose, K. Melting experiments on lherzolite KLB-1 under hydrous conditions and generation of high-magnesian andesitic melts. *Geology* **25**, 42–44 (1997).
47. Hirose, K. & Kawamoto, T. Hydrous partial melting of lherzolite at 1 GPa: the effect of H_2O on the genesis of basaltic magmas. *Earth Planet Sc. Lett.* **133**, 463–473 (1995).
48. Klingenberg, B. M. E. T. & Kushiro, I. Melting of a chromite-bearing harzburgite and generation of boninitic melts at low pressures under controlled oxygen fugacity. *Lithos* **37**, 1–14 (1996).
49. Kamenetsky, V. S., Sobolev, A. V., Eggins, S. M., Crawford, A. J. & Arculus, R. J. Olivine-enriched melt inclusions in chromites from low-Ca boninites, Cape Vogel, Papua New Guinea: evidence for ultramafic primary magma, refractory mantle source and enriched components. *Chem. Geol.* **183**, 287–303 (2002).
50. Kamenetsky, V. Methodology for the study of melt inclusions in Cr-spinel, and implications for parental melts of MORB from FAMOUS area. *Earth Planet Sc. Lett.* **142**, 479–486 (1996).
51. Schiano, P. et al. Primitive basaltic melts included in podiform chromites from the Oman ophiolite. *Earth Planet Sc. Lett.* **146**, 489–497 (1997).
52. Umino, S. et al. Thermal and chemical evolution of the subarc mantle revealed by spinel-hosted melt inclusions in boninite from the Ogasawara (Bonin) Archipelago, Japan. *Geology* **43**, 151–154 (2015).
53. Bell, A. S. et al. Chromium oxidation state in planetary basalts: oxygen fugacity indicator and critical variable for Cr-spinel stability. In *Lunar and Planetary Science Conference, No. JSC-CN-30566* (NTRS, The Woodlands, 2014).
54. Laubier, M., Schiano, P., Doucelance, R., Ottolini, L. & Laporte, D. Olivine-hosted melt inclusions and melting processes beneath the FAMOUS zone (mid-Atlantic ridge). *Chem. Geol.* **240**, 129–150 (2007).
55. Pollack, H. N. Cratonization and thermal evolution of the mantle. *Earth Planet Sc. Lett.* **80**, 175–182 (1986).
56. He, L. Thermal regime of the North China craton: implications for craton destruction. *Earth Sci. Rev.* **140**, 14–26 (2015).
57. Yin, A. An episodic slab-rollback model for the origin of the Tharsis rise on Mars: implications for initiation of local plate subduction and final unification of a kinematically linked global plate-tectonic network on Earth. *Lithosphere* **4**, 553–593 (2012).
58. Xin, G. Y. et al. Rapid transition from MORB-type to SSZ-type oceanic crust generation following subduction initiation: insights from the mafic dikes and metamorphic soles in the Pozantı–Karsantı ophiolite, SE Turkey. *Contrib. Mineral. Petrol.* https://doi.org/10.1007/s00410-021-01821-5 (2021).
59. Sobolev, A. V. & Danyusevsky, L. V. Petrology and geochemistry of boninites from the north termination of the tonga trench: constraints on the generation conditions of primary high-Ca boninite magmas. *J. Petrol.* **35**, 1183–1211 (1994).
60. Reagan, M. K. et al. Forearc ages reveal extensive short-lived and rapid seafloor spreading following subduction initiation. *Earth Planet Sc. Lett.* **506**, 520–529 (2019).

61. Li, J. et al. Reassessment of hydrofluoric acid desilicification in the carius tube digestion technique for Re–Os isotopic determination in geological samples. *Geostand. Geoanal. Res.* **39**, 17–30 (2015).
62. Ishikawa, A., Senda, R., Suzuki, K., Dale, C. W. & Meisel, T. Re-evaluating digestion methods for highly siderophile element and ^{187}Os isotope analysis: evidence from geological reference materials. *Chem. Geol.* **384**, 27–46 (2014).
63. Shervais, J. W. et al. Magmatic response to subduction initiation: part 1. Fore-arc basalts of the Izu–Bonin arc from IODP expedition 352. *Geochem. Geophy. Geosy.* **20**, 314–338 (2019).
64. Portnyagin, M., Hoernle, K. & Savelyev, D. Ultra-depleted melts from Kamchatkan ophiolites: Evidence for the interaction of the Hawaiian plume with an oceanic spreading center in the cretaceous? *Earth Planet Sc. Lett.* **287**, 194–204 (2009).
65. Xiong, F. et al. High-Al and high-Cr podiform chromitites from the western Yarlung–Zangbo suture zone, Tibet: implications from mineralogy and geochemistry of chromian spinel, and platinum-group elements. *Ore Geol. Rev.* **80**, 1020–1041 (2017).
66. Xiong, F. H. et al. Different type of chromitite and genetic model from Luobusa ophiolite Tibet. *Acta Petrol. Sin.* **30**, 2173–2163 (2014).
67. Xiong, Q. et al. Sulfide in dunite channels reflects long-distance reactive migration of mid-ocean-ridge melts from mantle source to crust: a Re–Os isotopic perspective. *Earth Planet Sc. Lett.* **531**, 115969 (2020).
68. Xiong, F. et al. Compositional and isotopic heterogeneities in the Neo-Tethyan upper mantle recorded by coexisting Al-rich and Cr-rich chromitites in the Purang peridotite massif, SW Tibet (China). *J. Asian Earth Sci.* **159**, 109–129 (2018).
69. Gervilla, F. et al. Distribution of platinum-group elements and Os isotopes in chromite ores from Mayarí–Baracoa ophiolitic belt (eastern Cuba). *Contrib. Mineral. Petrol.* **150**, 589–607 (2005).
70. Allan, J. F. Cr-spinel in depleted basalts from the Lau basin backard: petrogenetic history from Mg–Fe crystal–liquid exchange. In *Proc Ocean Drilling Program. Scientific Results* (eds. Hawkins, J., Parson, L., Allan, J. et al.) 565–583 (Ocean Drilling Program, College Station, 1994).

Acknowledgements

This study is supported by the National Key Research and Development Programme of China (2023YFF0804404), the National Natural Science Foundation of China (42372097, 42172074, and 91962217), the Fundamental Research Funds for Central Universities. We thank Nikko Pacle and Americus Perez for their assistance during the field excursion.

Author contributions

P.-F.Z., M.-F.Z., and G.P.Y.J. planned the field trip and conducted the sampling work. P..F.Z. did all the analyses of Os concentrations and isotopes with the assistance of J.L. in the lab. P.-F.Z., M.-F.Z., and C.Y.W. conceived the general idea and prepared the first draft of the manuscript. P.T.R., J.M., G.P.Y.J., and J.L. contributed to the critical discussion and improved the contents of the manuscript together. All the figures were newly designed and drawn by P.-F.Z.

Competing interests

The authors declare no competing interests.

Additional information

Supplementary information The online version contains supplementary material available at https://doi.org/10.1038/s41467-024-53508-7.

Correspondence and requests for materials should be addressed to Peng-Fei Zhang or Mei-Fu Zhou.

Peer review information *Nature Communications* thanks Ibrahim Uysal, Núria Pujol-Solà and the other, anonymous, reviewer(s) for their contribution to the peer review of this work. A peer review file is available.